http://mmg.tversu.ru ISSN 2311-1275

Mathematical Modelling and Geometry

Volume 2, No 1, p. 54 – 80 (2014)

Numerical solution of elliptic boundary-value problems for Schrödinger-type equations using the Kantorovich method

A.A. Gusev[1,a] **O. Chuluunbaatar**[1,2] **S.I. Vinitsky**[1]
A.G. Abrashkevich[3] **and V.L. Derbov**[4]

[1] Joint Institute for Nuclear Research, Dubna, Russia [2] National University of Mongolia, Ulaanbaatar, Mongolia [3] IBM Toronto Lab, Markham, Canada [4] Saratov State University, Saratov, Russia

e-mail: [a] gooseff@jinr.ru

Received 21 April 2014, in final form 29 April 2014. Published 30 April 2014.

Abstract. Calculation schemes for numerical solution of elliptic boundary-value problems for Schrödinger-type equations based on Kantorovich method that reduces the initial problem to a set of boundary-value problems for a system of ordinary second-order differential equations are presented. The reduced boundary-value problems are discretized using the high-accuracy finite element method and implemented in the form of program complexes in Fortran 77. The efficiency of the calculation schemes and programs is demonstrated by the analysis of benchmark calculations of a boundary-value problem with 3D Schrödinger equation, describing the bound states in the nonrelativistic helium atom. Physical results of the symbolic-numeric analysis of low-dimensional quantum models using the developed method and software are discussed.

Keywords: elliptic boundary-value problems, Schrödinger-type equations, Kantorovich method, finite element method, helium atom, low-dimensional quantum systems

PACS numbers: 02.30.Jr, 02.60.Lj, 31.15.Pf

The authors acknowledge the partial support from the Russian Foundation for Basic Research (grants No. 14-01-00420 and No. 13-01-00668), and the Joint Institute for Nuclear Research (theme 05-6-1119-2014/2016 "Methods, Algorithms and Software for Modeling Physical Systems, Mathematical Processing and Analysis of Experimental Data").

1. Introduction

The adiabatic approximation is an efficient tool for studying the dynamics of few-body quantum systems in physics of molecules, atoms, and atomic nuclei. The approximate separation of fast $\mathbf{x}_f$ and slow $\mathbf{x}_s$ variables in the Hamiltonian $H(\mathbf{x}_f, \mathbf{x}_s) = H_f(\mathbf{x}_f; \mathbf{x}_s) + H_s(\mathbf{x}_s)$, describing fast and slow subsystems with separated discrete energy spectra, and, correspondingly, in the expansion of the eigenfunction $\langle \mathbf{x}_f, \mathbf{x}_s | n_k \rangle$ in the basis functions $\langle \mathbf{x}_f | n'_{k+1}, \mathbf{x}_s \rangle$ of the Hamiltonian $H_f(\mathbf{x}_f; \mathbf{x}_s)$, depending on $\mathbf{x}_s$ as a parameter, i.e., the diagonal adiabatic approximation

$$\langle \mathbf{x}_f, \mathbf{x}_s | n_k \rangle = \sum\nolimits_{n'_{k+1}} \langle \mathbf{x}_f | n'_{k+1}, \mathbf{x}_s \rangle \langle \mathbf{x}_s, n'_{k+1} | n_k \rangle \approx \langle \mathbf{x}_f | n'_{k+1}, \mathbf{x}_s \rangle \langle \mathbf{x}_s, n'_{k+1} | n_k \rangle, \qquad (1)$$

was used, e.g., in the theory of electronic, vibrational and rotational spectra of molecules [1], in the dynamic theory of crystal lattice [2], in the method of generator coordinated for the cluster model of light nuclei [3].

Taking the nondiagonal terms into account with estimation of the expansion convergence rate (1) beyond any perturbation theory [2] corresponds to the reduction of the boundary-value problem to a set of coupled ordinary differential equations (ODE) of the second order in the Kantorovich method [4] that uses averaging of the problem over the set of eigenfunctions, depending on one of the independent variables as a parameter. In contrast to the diagonal (or adiabatic) approximation, this approach allows calculations with controllable precision [5, 6, 7, 8, 9], e.g., in the models of semiconductor quantum dots [10], or helium-like atoms and ions [11, 12, 13].

In the multidimensional case it is possible to apply the procedure of step-by-step averaging with sequential elimination of ordered independent variables $(\mathbf{x} = \{\mathbf{x}_f, \mathbf{x}_s\} = \{x_N \succ x_{N-1} \succ ... \succ x_1\}^T \in \mathbf{X} = \mathbf{X_N} \cup ... \cup \mathbf{X_1}$ in the subspace of the configuration space $\mathbf{X} \subset \mathbf{R}^N$)[14, 15], implemented, e.g., in the multistep adiabatic approximation for the model of coupled oscillators with ordered characteristic frequencies $\omega_f > \omega_s$, [16]. Note, that the step-by-step averaging procedure is close to the Marchuk's method of *coordinate-wise* splitting, however, it can be implemented using not only the projection methods of the Galerkin type, but also the multiparametric generalization of the Kantorovich method.

In spite of the complexity of its structure and implementation, the multiparametric Kantorovich method may offer an opportunity of more efficient exploitation of computer facilities, e.g., using MPI technology. The method is also expected to increase the precision of calculation of the parametric basis functions and the matrix elements of the ODE variable coefficients, expressed as integrals of basis functions and their derivatives with respect to parameters; it can also raise the convergence rate for the expansion of the desired solution [11, 12, 13].

The above motivation has determined the aim of this work: to present a general formulation of the multiparametric Kantorovich method (MPKM) and the symbolic-numeric algorithm for solving multidimensional boundary-value problems,

to analyze the efficiency of computational schemes and programs by the example of benchmark calculation of the ground and excited states of the nonrelativistic model of helium atom, and to discuss the physical results, obtained by symbolic-numerical analysis of low-dimensional model quantum systems using the proposed method and the elaborated software package.

The paper is organized as follows. Section 2 is devoted to the formulation of the MPKM theory and algorithm. In Section 3 the scheme of solving the boundary-value problem by means of the Kantorovich method (KM) is given. In Section 4 the analysis and the efficiency estimations for the benchmark calculations are presented. In Conclusion we briefly summarize the results obtained by the analysis of low-dimensional model quantum systems and discuss future implementation and possible applications of the method.

2. MPKM algorithm

Let us present the symbolic-numeric algorithm for multistep reduction of adiabatic equations, corresponding to multiparametric generalization of Kantorovich method, i.e., the reduction of a multidimensional boundary-value problem to ordinary differential equations, the solutions $\psi_{n_1}(\mathbf{x}) \in L^2(\mathbf{X})$, $\mathbf{X} \subset \mathbf{R}^N$ of which obey the appropriate boundary conditions [5]

$$\hat{H}\psi_{n_1}(\mathbf{x}) - 2E_{n_1}\psi_{n_1}(\mathbf{x}) = 0. \tag{2}$$

Here the Hamiltonian $\hat{H} = \sum_{i=1}^{N} \hat{H}_{N+1-i}$ of a quantum system, depending on the ordered variables $\mathbf{x} = \{x_N \succ x_{N-1} \succ ... \succ x_1\}^T \in \mathbf{X} \subset \mathbf{R}^N$, is represented by a sum of parametric Hamiltonians $\hat{H}_i \equiv \hat{H}_i(x_i; x_{i-1}, ..., x_1)$ of subsystems that depend upon the independent variable x_i and the set of parameters $x_{i-1}, ..., x_1$, the solutions satisfying the orthogonality and completeness conditions

$$\langle n_1'|n_1\rangle = \int_{\mathbf{X}} dx_N ... dx_1 \psi^{\dagger}_{n_1'}(\mathbf{x})\psi_{n_1}(\mathbf{x}) = \delta_{n_1' n_1}, \tag{3}$$

where δ_{ij} is the Kronecker symbol.

For solving the problem (2), (3) we propose a multistep generalization of the standard adiabatic expansion or Kantorovich reduction (1) in the following form:

$$\psi_{n_1}(\mathbf{x}) = \psi^{(1)}_{n_1}(x_N, ..., x_1) = \sum_{n_2''} \psi^{(2)}_{n_2''}(x_N, ..., x_2; x_1)\chi^{(1)}_{n_2'' n_1}(x_1) \tag{4}$$

$$= \sum_{n_3' n_2'} \psi^{(3)}_{n_3'}(x_N, ..., x_3; x_2, x_1)\chi^{(2)}_{n_3' n_2'}(x_2; x_1)\chi^{(1)}_{n_2' n_1}(x_1)$$

$$= \sum_{n_N' ... n_2'} \psi^{(N)}_{n_N'}(x_N; x_{N-1}, ..., x_1) ... \chi^{(k)}_{n_{k+1}' n_k'}(x_k; x_{k-1}, ..., x_1) ... \chi^{(2)}_{n_3' n_2'}(x_2; x_1)\chi^{(1)}_{n_2' n_1}(x_1),$$

where $\psi^{(k)}_{n_k}(x_N,...,x_k;x_{k-1},...,x_1)$ are solutions of auxiliary boundary-value problem with the Hamiltonians $\hat{H}^{(k)} \equiv \hat{H}^{(k)}(x_N,...,x_k;x_{k-1},...,x_1)$

$$\hat{H}^{(k)}\psi^{(k)}_{n_k} - \varepsilon^{(k)}_{n_k}\psi^{(k)}_{n_k} = 0, \quad \hat{H}^{(k)} = \sum_{i=N+1-k}^{N} \hat{H}_{N+1-i},$$

$$\langle n'_k|n_k\rangle = \int_{\mathbf{X_N}\cup...\cup\mathbf{X_{N+1-k}}} dx_N...dx_{N+1-k}\psi^{(k)\dagger}_{n'_k}\psi^{(k)}_{n_k} = \delta_{n'_k n_k}; \tag{5}$$

are determined by the recurrence relations

$$\psi^{(2)}_{n''_2}(x_N,...,x_2;x_1) = \sum_{n'_3}\psi^{(3)}_{n'_3}(x_N,...,x_3;x_2,x_1)\chi^{(2)}_{n'_3 n_2}(x_2;x_1),$$

$$\psi^{(k)}_{n_k}(x_N,...,x_k;x_{k-1},...,x_1) = \\ = \sum_{n'_{k+1}}\psi^{(k+1)}_{n'_{k+1}}(x_N,...,x_{k+1};x_k,...,x_1)\chi^{(k)}_{n'_{k+1}n_k}(x_k;x_{k-1},...,x_1).$$

Here required parametric solutions with respect to one of the independent variables $\langle n'_{k+1}|n_k\rangle \equiv \chi^{(k)}_{n'_{k+1}n_k}(x_k;x_{k-1},...,x_1)$ are determined by integrals of products of solutions of auxiliary boundary-value problems:
$\langle n'_{k+1}|n_k\rangle = \int_{\mathbf{X_N}\cup...\cup\mathbf{X_{k+1}}} dx_N...dx_{k+1}\psi^{(k+1)\dagger}_{n'_{k+1}}\psi^{(k)}_{n_k}$. Optimization of the convergence rate of the MPKM is possible for the appropriate ordering of the characteristic frequencies of the subsystems $\omega_N > \omega_{N-1} > ... > \omega_1$, where $\omega_k \simeq \max|\varepsilon^{(k)}_{n_k+1} - \varepsilon^{(k)}_{n_k}|$, with separated discrete spectra.

Below we present a symbolic MPKM algorithm for generating the boundary-value problem, implementing the multiparametric Kantorovich method (4) in the solution of the boundary-value problem (2) using the computer algebra system Maple. The examples of application of the typical versions of the algorithm are presented below.

The MPKM algorithm

Input:
$H = \sum_{i=1}^{N} H_{N+1-i}$ – the primary Hamiltonian depending on the ordered variables $\mathbf{x} = \{x_N \succ x_{N-1} \succ ... \succ x_1\}^T$, presented as a sum of parametric Hamiltonians $H_i \equiv H_i(x_i;x_{i-1},...,x_1)$, each depending on a single independent variable x_i and a set of parameters $x_{i-1},...,x_1$;
$H\psi_{n_1} - 2E_{n_1}\psi_{n_1} = 0$,
$\langle n'_1|n_1\rangle = \int_{\mathbf{X}} dx_N...dx_1\psi^{\dagger}_{n'_1}(\mathbf{x})\psi_{n_1}(\mathbf{x}) = \delta_{n'_1 n_1}$ is the primary eigenvalue problem
$\psi_{n_1} \equiv |n_1\rangle \leftrightarrow \langle\mathbf{x}|n_1\rangle \equiv \psi_{n_1}(\mathbf{x})$ and $2E_{n_1} = \varepsilon_{n_1}$.

Output:
Eq(k), $k = 1,...,N$, – the set of auxiliary parametric problems for calculating $\psi^{(k)}_{n_k} \equiv \psi^{(k)}_{n_k}(x_N,...,x_k;x_{k-1},...,x_1)$ and $\varepsilon^{(k)}_{n_k} \equiv \varepsilon^{(k)}_{n_k}(x_{k-1}...x_1)$, where $\psi_{n_1} = \psi^{(1)}_{n_1}$ and $2E_{n_1} = \varepsilon^{(1)}_{n_1}$ – the desired solutions of the primary eigenvalue problem.

Local:
$\psi^{(k)}_{n_k} \equiv \psi^{(k)}_{n_k}(x_N, ..., x_k; x_{k-1}, ..., x_1)$ and $\varepsilon_{n_k} \equiv \varepsilon^{(k)}_{n_k} \equiv \varepsilon^{(k)}_{n_k}(x_{k-1}...x_1)$ – the solutions of the auxiliary eigenvalue problem:
$(\sum_{i=N+1-k}^{N} H_{N+1-i})\psi^{(k)}_{n_k} - \varepsilon^{(k)}_{n_k}\psi^{(k)}_{n_k} = 0,$
$\langle n'_k|n_k\rangle = \int_{\mathbf{X_N}\cup...\cup\mathbf{X_{N+1-k}}} dx_N...dx_{N+1-k}\psi^{(k)\dagger}_{n'_k}\psi^{(k)}_{n_k} = \delta_{n'_k n_k};$
$\langle n'_{k+1}|n_k\rangle \equiv \chi^{(k)}_{n'_{k+1}n_k}(x_k; x_{k-1}, ..., x_1)$ – the auxiliary parametric solutions, defined by the relations:
$\langle n'_{k+1}|n_k\rangle = \int_{\mathbf{X_N}\cup...\cup\mathbf{X_{k+1}}} dx_N...dx_{k+1}\psi^{(k+1)\dagger}_{n'_{k+1}}\psi^{(k)}_{n_k},$
$\langle n_{k+1}|\Big[H_k, n'_{k+1}\rangle\Big] = \langle n_{k+1}|H_k n'_{k+1}\rangle - \langle n_{k+1}|n'_{k+1}\rangle H_k$, the square brackets $[,]$ denote a commutator.

1: Eq(N):=$\{H_{n_N}|n_N\rangle - \varepsilon_{n_N}|n_N\rangle = 0, \qquad \langle\psi^{(N)\dagger}_{n_N}|\psi^{(N)}_{n'_N}\rangle = \delta_{n_N n'_N}\}$
2: Eq(N) $\rightarrow\{|n_N\rangle, \varepsilon_{n_N}\}$
3: **for** $k := N-1 : 1$ step -1
4: Eq(k):=$\{(H_k + \varepsilon^{(k+1)}_{n_{k+1}} - \varepsilon^{(k)}_{n_k})\langle n_{k+1}|n_k\rangle$
$+ \sum_{n'_{k+1}} \langle n_{k+1}|\Big[H_k, n'_{k+1}\rangle\Big]\langle n'_{k+1}|n_k\rangle = 0\}.$
5: Eq(k) $\rightarrow\{\langle n'_{k+1}|n_k\rangle, \varepsilon^{(k)}_{n_k}\}$
6: $|n_k\rangle := \sum_{n'_{k+1}} |n'_{k+1}\rangle\langle n'_{k+1}|n_k\rangle$
7: **end for**
8: $\psi_{n_1} = |n_1\rangle$, $2E_{n_1} = \varepsilon^{(1)}_{n_1}$

Note, the expansion (1) is applied $N-1$ times from fastest x_N to lowest x_1 independent variables of set $\mathbf{x} = \{x_N \succ x_{N-1} \succ ... \succ x_1\}^T$ and involved in Step 6.

3. Kantorovich scheme for boundary-value problems

In a number of cases few-body quantum-mechanical problems can be reduced to the solution of boundary-value problems for the multidimensional time-independent Schrödinger equation [17, 18, 19, 20, 21, 22, 23, 24, 25]:

$$\hat{H}(z,\Omega)\Psi(z,\Omega) = E\Psi(z,\Omega), \quad \hat{H}(z,\Omega) = \hat{H}_1 + \frac{1}{f_3(z)}\hat{H}^{(2)}, \tag{6}$$
$$\hat{H}_1 = -\frac{1}{f_1(z)}\frac{\partial}{\partial z}f_2(z)\frac{\partial}{\partial z}, \quad \hat{H}^{(2)} = \left(-\hat{\Lambda}^2_\Omega + f_3(z)U(z,\Omega)\right).$$

Here $\hat{\Lambda}^2_\Omega$ is a self-adjoint differential operator of the elliptic type with partial derivatives in the finite domain $\hat{X} \subset \mathbf{R}^{d-1}$, $\Omega = \{\Omega_j\}_{j=1}^{d-1} \in \hat{X}$ is the set of independent variables, $z \in (z_1, z_2) \in B \subset \mathbf{R}^1$ is an independent variable, $X = B \otimes \hat{X} \subset \mathbf{R}^d$ is a finite domain of the coordinate space $\mathbf{R}^d$; E is a spectral parameter, corresponding to the energy of the quantum system. The functions $f_1(z) > 0$, $f_2(z) > 0$,

$f_3(z) > 0$, $\partial_z f_2(z)$, $U(z,\Omega)$ and $\partial_r U(r,\Omega)$ are assumed to be continuous and bounded for all $(r,\Omega) \in X$. It is also assumed that the self-adjoint operator $\hat{H}^{(2)}(\Omega;z) = -\hat{\Lambda}^2_\Omega + f_3(z)U(z,\Omega)$ has only a discrete real-valued spectrum $\boldsymbol{\varepsilon}(z)$. The solution $\Psi(z,\Omega) \in \mathbf{L}_2(X)$ of the equation (6) obeys the boundary conditions of the third kind:

$$\mu_l \frac{\partial \Psi(z_l,\Omega)}{\partial z} - \lambda_l \Psi(z,\Omega) = 0, \quad \Omega \in \partial\hat{X} \cup \hat{X}, \quad l = 1,2;$$
$$a\frac{\partial \Psi(z,\Omega)}{\partial \mathbf{n}} - b(z)\Psi(z,\Omega) = 0, \quad \Omega \in \partial\hat{X}, \quad z \in [z_1,z_2], \tag{7}$$

where μ_1, λ_1, μ_2, a are real constants; $\lambda_2 \equiv \lambda_2(z_2)$ is a real function, depending on z_2; $\mu_l^2 + \lambda_l^2 \neq 0$; the functions $b(z)$, $\partial_z b(z)$ are continuous and bounded; $\mathbf{n}$ is a unit vector normal to the boundary $\partial\hat{X}$ of the domain $\hat{X}$.

In the Kantorovich method (KM) the solution $\Psi(z,\Omega)$ is sought for in the form of an expansion in the single-parameter set of basis functions $\{\psi_j(\Omega;z)\}_{j=1}^{j_{\max}} \in \mathcal{F}_z \sim \mathbf{L}_2(\hat{X})$:

$$\Psi(z,\Omega) = \sum\nolimits_{j=1}^{j_{\max}} \psi_j^{(2)}(\Omega;z)\chi_{ji_o}^{(1)}(z). \tag{8}$$

In the expansion (8) the vector function $\boldsymbol{\chi}_{i_o}^{(1)}(z) = (\chi_{1i_o}^{(1)}(z),\ldots,\chi_{j_{\max}i_o}^{(1)}(z))^T$ is the one we seek for. The basis functions $\psi_j^{(2)}(\Omega;z)$ are solutions of the parametric eigenvalue problem

$$\hat{H}^{(2)}(\Omega;z)\psi_j^{(2)}(\Omega;z) = \varepsilon_j^{(2)}(z)\psi_j^{(2)}(\Omega;z), \tag{9}$$
$$a\frac{\partial \psi_j^{(2)}(\Omega;z)}{\partial \mathbf{n}} - b(z)\psi_j^{(2)}(\Omega;z) = 0,\ \Omega \in \partial\hat{X},\ z \in [z_1,z_2].$$

They form an orthonormal basis in the set of variables $\Omega \in \hat{X}$ for each value $z \in (z_1,z_2) \in B$:

$$\int_{\hat{X}} \psi_i^{(2)}(\Omega;z)\psi_j^{(2)}(\Omega;z)d\Omega = \delta_{ij}. \tag{10}$$

Here $\varepsilon_1^{(2)}(z) < \cdots < \varepsilon_{j_{\max}}^{(2)}(z) < \cdots \in \boldsymbol{\varepsilon}^{(2)}(z)$ is the desired set of real eigenvalues arranged in the ascending order.

By the projection (8)–(10) the problem (6), (7) is reduced to the bound-state problem (with respect to $E, \boldsymbol{\chi}^{(1)}(z)$) or to the multichannel scattering problem (with respect to $\{\lambda_{2,i_o}\}_{i_o=1}^{N_o}, \{\boldsymbol{\chi}_{i_o}(z)\}_{i_o=1}^{N_o}$, the value of E being fixed) for the system of $j_{\max}$ ordinary differential equations (ODE):

$$(\hat{\mathbf{H}}_1(z) + \hat{\mathbf{W}}^{(1)})\boldsymbol{\chi}^{(1)}(z) = E\boldsymbol{\chi}^{(1)}(z), \quad z \in (z_1,z_2) \tag{11}$$

with the boundary conditions of the third kind at the ends of the interval $z \in \bar{\Omega}_z = (z_1,z_2)$:

$$\mu_l\left(\mathbf{I}\frac{d}{dz} - \mathbf{Q}^{(1)}(z)\right)\boldsymbol{\chi}^{(1)}(z) - \lambda_l\boldsymbol{\chi}^{(1)}(z) = 0, \quad z = z_l, \quad l = 1,2 \tag{12}$$

where $\mathbf{I}$ is the unit matrix, $\hat{\mathbf{H}}(z)$ and $\hat{\mathbf{W}}^{(1)}$ are the self-adjoint matrix operators:

$$\hat{\mathbf{H}}_1(z) = -\frac{1}{f_1(z)}\mathbf{I}\frac{d}{dz}f_2(z)\frac{d}{dz}$$
$$\hat{\mathbf{W}}^{(1)} = \mathbf{V}(z) + \frac{f_2(z)}{f_1(z)}\mathbf{Q}^{(1)}(z)\frac{d}{dz} + \frac{1}{f_1(z)}\frac{d\,f_2(z)\mathbf{Q}^{(1)}(z)}{dz}. \quad (13)$$

The eigenfunction $\boldsymbol{\chi}^{(1)}(z)$ of the bound-state problem (11)–(13) is normalized:

$$\|\boldsymbol{\chi}^{(1)}(z)\|_0 = 1, \quad \|\boldsymbol{\chi}^{(1)}(z)\|_0^2 = \int_{z_1}^{z_2} f_1(z)\boldsymbol{\chi}^{(1)}(z)^T\boldsymbol{\chi}^{(1)}(z)dz. \quad (14)$$

For the multichannel scattering problem (11)–(13) on whole axis $z \in (-\infty, +\infty)$ the number of open channels $N_o = \max j \le j_{\max}$ is determined by the condition $E \ge \lim_{z_\pm\to\pm\infty} V_{jj}(z_\pm)$, if $\lim_{z_\pm\to\pm\infty} f_2(z_\pm)/f_1(z_\pm) = \text{const}$, and the normalization of the bounded solution $\boldsymbol{\Phi}^{(1)}(z) = \{\boldsymbol{\chi}_{i_o}^{(1)}(z)\}_{i_o=1}^{N_o}$ by the condition at $z_+ \to +\infty$ and $z_- \to -\infty$ we use

$$\begin{pmatrix} \boldsymbol{\Phi}_\rightarrow(z_+) & \boldsymbol{\Phi}_\leftarrow(z_+) \\ \boldsymbol{\Phi}_\rightarrow(z_-) & \boldsymbol{\Phi}_\leftarrow(z_-) \end{pmatrix} = \begin{pmatrix} \mathbf{0} & \mathbf{X}^{(-)}(z_+) \\ \mathbf{X}^{(+)}(z_-) & \mathbf{0} \end{pmatrix} + \begin{pmatrix} \mathbf{0} & \mathbf{X}^{(+)}(z_+) \\ \mathbf{X}^{(-)}(z_-) & \mathbf{0} \end{pmatrix}\mathbf{S}, \quad (15)$$

where $\mathbf{X}^{(\pm)}(z)$ are asymptotic rectangle-matrix solutions of dimension $j_{\max} \times N_o$ derived in [24] and $\mathbf{S}$ is the symmetric and unitary scattering matrix

$$\mathbf{S} = \begin{pmatrix} \mathbf{R}_\rightarrow & \mathbf{T}_\leftarrow \\ \mathbf{T}_\rightarrow & \mathbf{R}_\leftarrow \end{pmatrix} \quad (16)$$

which is composed of the reflection $\mathbf{R}_\rightarrow$, $\mathbf{R}_\leftarrow$ and transmission $\mathbf{T}_\rightarrow$, $\mathbf{T}_\leftarrow$ amplitude matrices of dimension $N_o \times N_o$, subscripts $\rightarrow$ and $\leftarrow$ denote the initial direction of the particle motion along the z axis [7, 24].

For the multichannel scattering problem (11)–(13) on semiaxis $z \in (0, +\infty)$, instead of (15) one has

$$\boldsymbol{\Phi}^{(1)}(z_+) = \boldsymbol{\Phi}_{\text{reg}}^{(1)}(z_+) + \boldsymbol{\Phi}_{\text{irr}}^{(1)}(z_+)\mathbf{K}, \quad (17)$$

where $\mathbf{K}$ is the desired scattering matrix having the dimension $N_o \times N_o$, $\boldsymbol{\Phi}_{\text{reg}}^{(1)}(z)$ and $\boldsymbol{\Phi}_{\text{irr}}^{(1)}(z)$ are the asymptotic expressions of dimension $j_{\max} \times N_o$ for regular and irregular solutions of Eq. (11), derived in Ref. [17, 18].

In Eqs. (13) the variable elements of the matrices $\mathbf{V}(z)$ and $\mathbf{Q}^{(1)}(z)$ having the dimension $j_{\max} \times j_{\max}$ are expresses in terms of the solutions of the problem (9) and their derivatives with respect to the parameter:

$$V_{ij}(z) = V_{ji}(z) = \frac{\varepsilon_i^{(2)}(z) + \varepsilon_j^{(2)}(z)}{2f_3(z)}\delta_{ij} + \frac{f_2(z)}{f_1(z)}H_{ij}^{(1)}(z),$$
$$H_{ij}^{(1)}(z) = H_{ji}^{(1)}(z) = \int_{\hat{X}} \frac{\partial\psi_i^{(2)}(\Omega;z)}{\partial z}\frac{\partial\psi_j^{(2)}(\Omega;z)}{\partial z}d\Omega, \quad (18)$$
$$Q_{ij}^{(1)}(z) = -Q_{ji}^{(1)}(z) = -\int_{\hat{X}} \psi_i^{(2)}(\Omega;z)\frac{\partial\psi_j^{(2)}(\Omega;z)}{\partial z}d\Omega.$$

Differentiation with respect to the parameter of the problem (9), (10) leads to the inhomogeneous boundary-value problem with respect to the desired parameter derivative $\partial_z \psi_j(\Omega; z) \in \mathcal{F}_r \sim \mathbf{L}_2(\hat{X})$:

$$\left(\hat{H}^{(2)}(\Omega; z) - \varepsilon_j^{(2)}(z)\right) \frac{\partial \psi_j^{(2)}(\Omega; z)}{\partial z} = \left(\frac{\partial \varepsilon_j^{(2)}(z)}{\partial z} - \frac{\partial \hat{H}^{(2)}(\Omega; z)}{\partial z}\right) \psi_j^{(2)}(\Omega; z), \quad (19)$$

$$a \frac{\partial^2 \psi_j^{(2)}(\Omega; z)}{\partial \mathbf{n} \partial z} - b(z) \frac{\partial \psi_j^{(2)}(\Omega; z)}{\partial z} = \frac{\partial b(z)}{\partial z} \psi_j^{(2)}(\Omega; r), \; \Omega \in \partial \hat{X}, \; z \in [z_1, z_2],$$

$$\int_{\hat{X}} \psi_j^{(2)}(\Omega; z) \frac{\partial \psi_j^{(2)}(\Omega; z)}{\partial z} d\Omega = 0.$$

The implementation of MK requires efficient calculation schemes for solving the following problems.

1. Calculation of a finite set of eigenvalues and eigenfunctions of the parametric boundary-value problem (9), (10).

2. Calculation of the first derivative of eigenfunctions with respect to the parameter from the inhomogeneous boundary-value problem (19).

3. Calculation of the elements of matrices $\mathbf{Q}^{(1)}(z)$ and $\mathbf{V}(z)$ using the formulae (18).

4. Solution of the bound-state problem for the set of ODE (11)–(14).

5. Solution of the multichannel scattering problem for the set of ODE (11)–(13), (17).

For solving the problems **1**–**5** numerically the efficient variation-projection computational schemes and economic algorithms [25, 26] were developed basing on the **R**-matrix theory, asymptotic methods and the finite element method (FEM). The problem-oriented software packages KANTBP [5, 6, 7], POTHMF [27], ODPEVP [8], and POTHEA [28] were elaborated.

The software package KANTBP is intended for numerical solution of the problems **4** and **5**. The constructed numerical scheme provides the known estimates of the following errors of the numerical solution on the nonuniform mesh $\Omega^p_{z_h}[z_1, z_2]$:

$$\left| E_j - E_j^h \right| \le c_1 h^{2p}, \quad \left\| \boldsymbol{\chi}_j^{(1)}(z) - \boldsymbol{\chi}_j^{h(1)} \right\|_0 \le c_2 h^{p+1}, \quad (20)$$

where E_j and $\boldsymbol{\chi}_j^{(1)}(z) \in \mathcal{H}^2$ are the desired eigenvalues and the corresponding eigenfunctions of the bound-state problem; E_j^h and $\boldsymbol{\chi}_j^{h(1)} \in \mathcal{H}^1$ are the corresponding numerical solutions; h is the maximal pitch of the finite-element mesh $\Omega^p_{z_h}[z_1, z_2]$; p is the order of approximation; c_1 and c_2 are positive constants independent of h and p. Similar estimates are valid also for the numerical solution of the multichannel scattering problem, where λ_j^h are the eigenvalues of the reaction matrix and $\boldsymbol{\chi}_j^{h(1)}$ are the corresponding eigenfunctions.

The software package ODPEVP within the problems **1**–**3** is intended for numerical solution of the single-parameter Sturm-Liouville problem in the finite

interval $x \in \bar{\Omega}_x = (x_1, x_2)$:

$$\hat{H}^{(2)}(x;z)\psi_j^{(2)}(x;z) = \epsilon_j^{(2)}(z)\psi_j^{(2)}(x;z)$$
$$\hat{H}^{(2)}(x;z) = -\frac{1}{g_1(x)}\frac{d}{dx}g_2(x)\frac{d}{dx} + f_3(z)U(z,x). \tag{21}$$

Here $z \in \Omega_z = [z_1, z_2]$ is a real parameter, $\epsilon_j(z)$ are the eigenvalues, depending on the parameter z. The functions $g_1(x) > 0$, $g_2(x) > 0$, $d_x g_2(x)$, $U(z,x)$, and $\partial_z U(z,x)$ are assumed to be continuous and bounded at all $x \in \bar{\Omega}_x$ and $z \in \Omega_z$. The parametric eigenfunctions $\psi_j^{(2)}(x;z)$ obey the boundary conditions of the third kind at the boundary points of the interval $x \in \bar{\Omega}_x$:

$$a_l g_2(x)\frac{d\psi_j^{(2)}(x;z)}{dx} + b_l(z)\psi_j^{(2)}(x;z) = 0, \quad x = x_l, \quad l = 1,2, \tag{22}$$

and satisfy the normalization condition

$$\|\psi_j(x;z)\|_0 = 1, \quad \|v(x)\|_0^2 = \int_{x_1}^{x_2} g_1(x)v(x)^2 dx. \tag{23}$$

Here $a_1 \geq 0$, $a_2 \geq 0$ are real constants, the functions $b_1(z) \leq 0$, $b_2(z) \geq 0$, $\partial_z b_1(z)$ and $\partial_z b_2(z)$ are continuous and bounded at $z \in \Omega_z$, $a_l^2 + b_l^2(z) \neq 0$.

An economic algorithm providing the prescribed accuracy was proposed for the calculating the set of $j_{\max}$ eigenvalues $\epsilon_j^{(2)}(z)$, eigenfunctions $\psi_i^{(2)}(x;z)$, their derivatives $\frac{\partial\epsilon_j^{(2)}(z)}{\partial z}$, $\frac{\partial\psi_i^{(2)}(x;z)}{\partial z}$ with respect to the parameter z, and the integrals

$$H_{ij}^{(1)}(z) = \int_{x_1}^{x_2} g_1(x)\frac{\partial\psi_i^{(2)}(x;z)}{\partial z}\frac{\partial\psi_j^{(2)}(x;z)}{\partial z}dx, \tag{24}$$
$$Q_{ij}^{(1)}(z) = -\int_{x_1}^{x_2} g_1(x)\psi_i^{(2)}(x;z)\frac{\partial\psi_j^{(2)}(x;z)}{\partial z}dx.$$

In the FEM for the numerical solution $\epsilon_j^{h(2)}$ and $\boldsymbol{\psi}_j^{h(2)}$ the following estimates of the errors are proved:

$$\left|\epsilon_j^{(2)}(x) - \epsilon_j^{h(2)}\right| \leq c_1 h^{2p}, \quad \left\|\psi_j^{(2)}(x;z) - \boldsymbol{\psi}_j^{h(2)}\right\|_0 \leq c_2 h^{p+1}, \tag{25}$$

where $\epsilon_j^{(2)}(z)$ and $\psi_j^{(2)}(x;z) \in \mathcal{H}^2$ are the precise solutions; $\epsilon_j^{h(1)}$ and $\boldsymbol{\psi}_j^{h(2)} \in \mathcal{H}^1$ are the corresponding numerical solutions; h is the maximal pitch of the finite-element mesh $\Omega_{x_h}^p[x_{\min}, x_{\max}]$; p is the order of approximation; c_1 and c_2 are positive constants independent of h and p.

It is proved that the following estimate takes place [26]:

Theorem. *For a given value of the parameter z the errors of approximation for the first derivatives of eigenvalues, eigenfunctions of the boundary-value problem*

(21), (22), and the integrals (24) with respect to the parameter are bounded by the following inequalities:

$$\left|\frac{\partial\epsilon_j^{(2)}(z)}{\partial z}-\frac{\partial\epsilon_j^{h(2)}}{\partial z}\right|\le c_3h^{2p},\quad \left\|\frac{\partial\psi_j^{(2)}(x;z)}{\partial z}-\frac{\partial\boldsymbol{\psi}_j^{h(2)}}{\partial z}\right\|_0\le c_4h^{p+1},\tag{26}$$
$$\left|Q_{ij}^{(1)}(z)-Q_{ij}^{h(1)}\right|\le c_5h^{2p},\quad \left|H_{ij}^{(1)}(z)-H_{ij}^{h(1)}\right|\le c_6h^{2p},$$

where $\partial_z\epsilon_j^{(2)}(z)$ *and* $\partial_z\psi_j^{(2)}(x;z)\in\mathcal{H}^2$, $Q_{ij}^{(1)}(z)$ *and* $H_{ij}^{(1)}(z)$ *are the exact functions;* $\partial_z\epsilon_j^{h(2)}$ *and* $\partial_z\boldsymbol{\psi}_j^{h(2)}\in\mathcal{H}^1$, $Q_{ij}^{h(1)}$ *and* $H_{ij}^{h(1)}$ *are the corresponding numerical values;* c_3, c_4, c_5 *and* c_6 *are positive constants independent of* h *and* p.

Within the framework of the problems **1**–**3** the program POTHEA is intended for the numerical solution of the the parametric 2D BVP for a self-adjoint second-order elliptic differential equation with respect to $\mathbf{x}=\{x_2=y\succ x_1=x\}^T\in\mathbf{X}\subset\mathbf{R}^2$ in the two-dimensional domain $\Omega=[x_{\min},x_{\max}]\times[y_{\min},y_{\max}]$

$$\left(\hat{H}^{(2)}(x,y;z)-\varepsilon_i^{(2)}(z)\right)\psi_i^{(2)}(x,y;z)=0,\tag{27}$$
$$\hat{H}^{(2)}(x,y;z)=\hat{H}_2(y;z)+\frac{1}{g_3(y)}\hat{H}^{(3)}(x;y,z),$$
$$\hat{H}_2(y;z)=-\frac{1}{g_1(y)}\frac{\partial}{\partial y}g_2(y)\frac{\partial}{\partial y}$$
$$\hat{H}^{(3)}(x;y,z)=-\frac{1}{g_4(x)}\frac{\partial}{\partial x}g_5(x)\frac{\partial}{\partial x}+f_3(z)g_3(y)U(x,y;z)$$

with the Dirichlet and/or Neumann boundary conditions

$$\lim_{y\to y_t}f_2(y)\partial_y\psi_i^{(2)}(x,y;z)=0\text{ or }\psi_i^{(2)}(x,y_t;z)=0,\ x\in(x_{\min},x_{\max}),\tag{28}$$
$$\lim_{x\to x_t}f_5(x)\partial_x\psi_i^{(2)}(x,y;z)=0\text{ or }\psi_i^{(2)}(x_t,y;z)=0,\ y\in[y_{\min},y_{\max}],$$

where $t=\min,\max$ and $\partial_y\equiv\frac{\partial}{\partial y}$. Here $z\in[z_{\min},z_{\max}]$ is a parameter, the functions $g_1(y)>0$, $g_2(y)>0$, $g_3(y)>0$, $g_4(x)>0$, $g_5(x)>0$, and $\partial_yg_2(y)$, $\partial_xg_5(x)$, $U(x,y;z)$, $\partial_zU(x,y;z)$ are continuous in $(x,y)\in\Omega/\partial\Omega$. It is also assumed that the parametric boundary-value problem (27), (28) has only a discrete spectrum.

The program executes the following steps.

In **Step 1** with the required accuracy of the order similar to (25) the program calculates a set of $j_{\max}$ smallest eigenvalues $\varepsilon_1^{(2)}(z)<\varepsilon_2^{(2)}(z)<\ldots\varepsilon_N^{(2)}(z)$, and $\varepsilon_1^{(2)}(z)\alpha(z)$, and the corresponding eigenfunctions $\{\psi_j^{(2)}(x,y;z)\}_{j=1}^N\in F_z\sim\mathbf{L}_2(\Omega_{x,y})$, satisfying the orthogonality and normalization conditions

$$\int_{y_{\min}}^{y_{\max}}dy\,g_1(y)\int_{x_{\min}}^{x_{\max}}dx\,g_4(x)\psi_i^{(2)}(x,y;z)\psi_j^{(2)}(x,y;z)=\delta_{ij},\tag{29}$$

where $\alpha(z)>-\infty$ is the lower bound of the smallest eigenvalue of $\varepsilon_1^{(2)}(z)$.

In **Step 2** the program computes a set of partial derivatives of the eigenvalues $\partial\varepsilon_j^{(2)}(z)/\partial z$ and eigenfunctions $\partial\psi_j^{(2)}(x,y;z)/\partial z$ with the accuracy of the same order as achieved for the eigenvalues and eigenfunctions of the BVP (27)–(29), respectively.

In **Step 3** the program computes the matrix elements defined by the integrals

$$H_{ij}^{(1)}(z) = H_{ji}^{(1)}(z) = \int\limits_{y_{\min}}^{y_{\max}} dy\, g_1(y) \int\limits_{x_{\min}}^{x_{\max}} dx\, g_4(x)\partial_z\psi_i^{(2)}(x,y;z)\partial_z\psi_j^{(2)}(x,y;z), \quad (30)$$

$$Q_{ij}^{(1)}(z) = -Q_{ji}^{(1)}(z) = -\int\limits_{y_{\min}}^{y_{\max}} dy\, g_1(y) \int\limits_{x_{\min}}^{x_{\max}} dx\, g_4(x)\psi_i^{(2)}(x,y;z)\partial_z\psi_j^{(2)}(x,y;z).$$

with the accuracy of the same order as achieved for the corresponding eigenvalues $\varepsilon(z)$ of the BVP (27)–(29) similar to (26).

Reduction of the parametric 2D BVP to parametric 1D BVPs

Step 1.1. The partial wave function $\psi_i^{(2)}(x,y;z)$ is expanded over the orthonormal basis $\{\psi_j^{(3)}(x)\}_{j=1}^{j_{\max}}$ $(j_{\max}\to\infty)$ in the conventional (C) form

$$\psi_i^{(2)}(x,y;z) = \sum_{j=1}^{j_{\max}} \psi_j^{(3)}(x)\chi_{ji}^{(2)}(y;z), \quad (31)$$

or $\{\psi_j^{(3)}(x;y,z)\}_{j=1}^{j_{\max}}$ $(j_{\max}\to\infty)$ in the Kantorovich (K) form

$$\psi_i^{(2)}(x,y;z) = \sum_{j=1}^{j_{\max}} \psi_j^{(3)}(x;y,z)\chi_{ji}^{(2)}(y;z). \quad (32)$$

In Eq. (31) the vector functions $\boldsymbol{\chi}_i^{(2)}(y;z) = (\chi_{1i}(y;z),\ldots,\chi_{j_{\max}i}(y;z))^T$ are unknown.

Step 1.1.1. If solution is sought in the C form then the functions $\psi_j^{(3)}(x)$ are determined as solutions of the following eigenvalue problem:

$$\left(-\frac{1}{g_4(x)}\frac{d}{dx}g_5(x)\frac{d}{dx} + U_0(x)\right)\psi_j^{(3)}(x) = \varepsilon_j^{(3)}\psi_j^{(3)}(x), \quad (33)$$

with the Dirichlet and/or Neumann type boundary conditions

$$\lim_{x\to x_t} g_5(x)\frac{d\psi_j^{(3)}(x)}{dx} = 0 \quad \text{or} \quad \psi_j^{(3)}(x_t) = 0, \quad (34)$$

where $t = \min, \max$ and $U_0(x)$ is a known function and

$$\int_{x_{\min}}^{x_{\max}} dx\, g_4(x)\psi_i^{(3)}(x)\psi_j^{(3)}(x) = \delta_{ij}. \quad (35)$$

Step 1.1.2. If solution is sought in the K form then the functions $\psi_j^{(3)}(x;y,z)$ are determined as solutions of the following eigenvalue problem:

$$\hat{H}_3(x;y,z)\psi_j^{(3)}(x;y,z) = \varepsilon_j^{(3)}(y,z)\psi_j^{(3)}(x;y,z),$$
$$\hat{H}_3(x;y,z) = \left(-\frac{1}{g_4(x)}\frac{d}{dx}g_5(x)\frac{d}{dx} + f_3(z)g_3(y)U(x;y,z)\right) \tag{36}$$

with the Dirichlet and/or Neumann type boundary conditions

$$\lim_{x\to x_t} g_5(x)\frac{d\psi_j^{(3)}(x;y,z)}{dx} = 0 \quad \text{or} \quad \psi_j^{(3)}(x_t;y,z) = 0, \tag{37}$$

where $t = \min, \max$ and $U(x,y;z)$ is a known function of the original problem (27) and orthonormalization conditions

$$\int_{x_{\min}}^{x_{\max}} dx\, g_4(x)\psi_i^{(3)}(x;y,z)\psi_j^{(3)}(x;y,z) = \delta_{ij}. \tag{38}$$

Note, that these problems can be numerically solved with the given accuracy by means of the ODPEVP program [8].

Step 1.1.3. If solution is sought in the K form then taking a derivative of the boundary problem (36)–(38) with respect to parameter $\bullet = y$ or $\bullet = z$, we get that $\partial_y\psi_i^{(3)}(x;y,z)$ or $\partial_z\psi_i^{(3)}(x;y,z)$ can be obtained as a solution of the following parametric inhomogeneous BVPs:

$$\left(\hat{H}_3(x;y,z) - \varepsilon_i^{(3)}(y,z)\right)\frac{\partial\psi_i^{(3)}(y;z)}{\partial\bullet} =$$
$$= -\left[\frac{\partial}{\partial\bullet}\left(f_3(z)g_3(y)U(x;y,z) - \varepsilon_i^{(3)}(y,z)\right)\right]\psi^{(i)}(x;y,z), \tag{39}$$

with the Dirichlet and/or Neumann type boundary conditions

$$\lim_{y\to y_t} g_5(x)\frac{\partial[\frac{\partial\psi_i^{(3)}(x;y,z)}{\partial x}]}{\partial\bullet} = 0 \quad \text{or} \quad \frac{\partial\psi_i^{(3)}(x;y,z)}{\partial\bullet} = 0, \tag{40}$$

where $t = \min, \max$ and $\partial_\bullet \equiv \frac{\partial}{\partial\bullet}$. The parametric BVP (39), (40) has a unique solution if and only if the conditions are fulfilled

$$\int_{x_{\min}}^{x_{\max}} dy g_4(x)\psi_i^{(3)}(x;y,z)\frac{\partial\psi_i^{(3)}(x;y,z)}{\partial\bullet} = 0, \tag{41}$$

$$\frac{\partial\varepsilon_i^{(3)}(y,z)}{\partial\bullet} = \int_{x_{\min}}^{x_{\max}} dy\, g_4(x)\psi_i^{(3)}(x;y,z)\frac{\partial U(x;y,z)}{\partial\bullet}\psi_i^{(3)}(x;y,z). \tag{42}$$

and matrix elements $H_{ij}^{(2)}(y,z,\partial_\bullet)$ and $Q_{ij}^{(2)}(y,z,\partial_\bullet)$ defined by integrals

$$H_{ij}^{(2)}(y,z,\partial_\bullet) = H_{ji}^{(2)}(y,z,\partial_\bullet) = \int_{x_{\min}}^{x_{\max}} dx\, g_4(x)\frac{\partial\psi_i^{(3)}(x;y,z)}{\partial\bullet}\frac{\partial\psi_j^{(3)}(x;y,z)}{\partial\bullet}, \tag{43}$$

$$Q_{ij}^{(2)}(y,z,\partial_\bullet) = -Q_{ji}^{(2)}(y,z,\partial_\bullet) = -\int_{x_{\min}}^{x_{\max}} dx\, g_4(x)\,\psi_i^{(3)}(x;y,z)\frac{\partial\psi_j^{(3)}(x;y,z)}{\partial\bullet}.$$

Note, these problems are numerically solved with a given accuracy by means of the ODPEVP program [8].

Step 1.2. After minimizing the Rayleigh-Ritz variational functional and using the expansion (31), the parametric BVP (27)–(29) is reduced to a finite set of $j_{\max}$ ODEs (in C or K forms)

$$\left(\hat{\mathbf{H}}^{(\mathbf{2})}(y;z) - \varepsilon_i^{(2)}(z)\,\mathbf{I}\right)\boldsymbol{\chi}_i^{(2)}(y;z) = 0, \tag{44}$$

$$\hat{\mathbf{H}}^{(\mathbf{2})}(y;z) = -\frac{1}{g_1(y)}\mathbf{I}\frac{\partial}{\partial y}g_2(y)\frac{\partial}{\partial y} + \mathbf{W}^{(2)}(y;z)$$

$$\lim_{y\to y_t} g_2(y)\frac{\partial \boldsymbol{\chi}_i^{(2)}(y;z)}{\partial y} = 0 \quad \text{or} \quad \boldsymbol{\chi}_i^{(2)}(y_t;z) = 0, \tag{45}$$

$$I_{ij} = \delta_{ij} = \int_{y_{\min}}^{y_{\max}} dy\, g_1(y)\left(\boldsymbol{\chi}_i^{(2)}(y;z)\right)^T \boldsymbol{\chi}_j^{(2)}(y;z), \tag{46}$$

Here in the C form, $\mathbf{I}$ and $\mathbf{W}^{(2)}(y;z)$ are symmetric matrices of the dimension $j_{\max}\times j_{\max}$

$$W_{ij}^{(2)}(y;z) = \frac{\varepsilon_i^{(3)} + \varepsilon_j^{(3)}}{2g_3(y)}\delta_{ij} + f_3(z)V^c(y;z) - f_3(z)\frac{V^d}{g_3(y)},$$

$$V^c(y;z) = \int_{x_{\min}}^{x_{\max}} dx\, g_4(x)\,\psi_i^{(3)}(x)U(x,y;z)\psi_j^{(3)}(x) \tag{47}$$

$$V^d = \int_{x_{\min}}^{x_{\max}} dx\, g_4(x)\,\psi_i^{(3)}(x)U_0(x)\psi_j^{(3)}(x)$$

while in the K form $\mathbf{W}^{(2)}(y,z) \equiv \mathbf{W}^{(2)}(y,z,\partial_y)$ is a self-adjoint matrix differential operator of the dimension $j_{\max}\times j_{\max}$

$$W_{ij}^{(2)}(y,z,\partial_y) = \frac{\varepsilon_i^{(3)}(y,z) + \varepsilon_j^{(3)}(y,z)}{2g_3(y)}\delta_{ij} + \frac{g_2(y)}{g_1(y)}H_{ij}^{(2)}(y,z,\partial_y) \tag{48}$$

$$+\frac{1}{g_1(y)}\left(\frac{\partial}{\partial y}[g_2(y)Q_{ij}^{(2)}(y,z,\partial_y)]\right) + \frac{g_2(y)}{g_1(y)}Q_{ij}^{(2)}(y,z,\partial_y))\frac{\partial}{\partial y},$$

with $H_{ij}^{(2)}(y,z,\partial_y)$ and $Q_{ij}^{(2)}(y,z,\partial_y)$ defined by formula (43) were calculated on **step** 1.1.3. with a given accuracy by means of the ODPEVP program [8].

Step 2. Taking a derivative of the boundary problem (44)–(46) with respect to parameter z, we get that $\partial_z\boldsymbol{\chi}_i^{(2)}(y;z)$ can be obtained as a solution of the following parametric inhomogeneous BVP:

$$\left(\hat{\mathbf{H}}^{(\mathbf{2})}(y;z) - \varepsilon_i^{(2)}(z)\,\mathbf{I}\right)\frac{\partial \boldsymbol{\chi}_i^{(2)}(y;z)}{\partial z} = -\left[\frac{\partial}{\partial z}\left(\mathbf{W}^{(2)}(y;z) - \varepsilon_i^{(2)}(z)\,\mathbf{I}\right)\right]\boldsymbol{\chi}_i^{(2)}(y;z), \tag{49}$$

with the Dirichlet and/or Neumann type boundary conditions

$$\lim_{y\to y_t} g_2(y)\frac{\partial[\frac{\partial \boldsymbol{\chi}_i^{(2)}(y;z)}{\partial z}]}{\partial y}=0 \quad \text{or} \quad \frac{\partial \boldsymbol{\chi}_i^{(2)}(y_t;z)}{\partial z}=0, \tag{50}$$

where $t=\min,\max$ and $\partial_y\equiv\frac{\partial}{\partial y}$. The parametric BVP (49), (50) has a unique solution if and only if the following conditions are satisfied

$$\int_{y_{\min}}^{y_{\max}} dy g_1(y)\left(\boldsymbol{\chi}_i^{(2)}(y;r)\right)^T\frac{\partial \boldsymbol{\chi}_i^{(2)}(y;z)}{\partial z}=0, \tag{51}$$

$$\frac{\partial \varepsilon_i^{(2)}(z)}{\partial z}=\int_{y_{\min}}^{y_{\max}} dy\, g_1(y)\left(\boldsymbol{\chi}_i^{(2)}(y;z)\right)^T\frac{\partial \mathbf{W}^{(2)}(y;z)}{\partial z}\boldsymbol{\chi}_i^{(2)}(y;z). \tag{52}$$

Step 3. The required matrix elements (30) are represented by the integrals in the C form

$$H_{ij}^{(1)}(z)=H_{ji}^{(1)}(z)=\int_{y_{\min}}^{y_{\max}} dy\, g_1(y)\left(\frac{\partial \boldsymbol{\chi}_i^{(2)}(y;z)}{\partial z}\right)^T\frac{\partial \boldsymbol{\chi}_j^{(2)}(y;z)}{\partial z}, \tag{53}$$

$$Q_{ij}^{(1)}(z)=-Q_{ji}^{(1)}(z)=-\int_{y_{\min}}^{y_{\max}} dy\, g_1(y)\left(\boldsymbol{\chi}_i^{(2)}(y;z)\right)^T\frac{\partial \boldsymbol{\chi}_j^{(2)}(y;z)}{\partial z},$$

and by the integrals in the K form

$$\begin{aligned}
H_{ij}^{(1)}(z)=H_{ji}^{(1)}(z)&=\int_{y_{\min}}^{y_{\max}} dy\, g_1(y)(\partial_z\boldsymbol{\chi}_i^{(2)}(y;z))^T\partial_z\boldsymbol{\chi}_j^{(2)}(y;z)\\
&+\int_{y_{\min}}^{y_{\max}} dy\, g_1(y)(\partial_z\boldsymbol{\chi}_i^{(2)}(y;z))^T\mathbf{Q}^{(2)}(y;z,\partial_z)\boldsymbol{\chi}_j^{(2)}(y;z)\\
&-\int_{y_{\min}}^{y_{\max}} dy\, g_1(y)(\boldsymbol{\chi}_i^{(2)}(y;z))^T\mathbf{Q}^{(2)}(y;z,\partial_z)(\partial_z\boldsymbol{\chi}_j^{(2)}(y;z))\\
&+\int_{y_{\min}}^{y_{\max}} dy\, g_1(y)(\boldsymbol{\chi}_i^{(2)}(y;z))^T)\mathbf{H}^{(2)}(y;z,\partial_z)\boldsymbol{\chi}_j^{(2)}(y;z),\\
Q_{ij}^{(1)}(z)=-Q_{ji}^{(1)}(z)&=\int_{y_{\min}}^{y_{\max}} dy\, g_1(y)\boldsymbol{\chi}_i^{(2)}(y;z))^T\mathbf{Q}^{(2)}(y;z,\partial_z)\boldsymbol{\chi}_j^{(2)}(y;z)\\
&-\int_{y_{\min}}^{y_{\max}} dy\, g_1(y)\boldsymbol{\chi}_i^{(2)}(y;z))^T\partial_z\boldsymbol{\chi}_j^{(2)}(y;z),
\end{aligned} \tag{54}$$

where $\mathbf{H}^{(2)}(y;z,\partial_z) = \{H^{(2)}_{i'j'}(y;z,\partial_z)\}$ and $\mathbf{Q}^{(2)}(y;z,\partial_z) = \{Q^{(2)}_{i'j'}(y;z,\partial_z)\}$ defined by formula (43) were calculated on **step** 1.1.3. with a given accuracy by means of the ODPEVP program [8].

The calculated eigenvalues $\varepsilon^{(1)}_i(z)$ and matrix elements $H^{(1)}_{ij}(z)$, $Q^{(1)}_{ij}(z)$ can be used for solving bound-state and multichannel scattering problems for a system of coupled ODEs with respect to the variable z with the help of the KANTBP program [5, 6, 7].

3.1 Continuity conditions for the eigenfunction $\psi^{(2)}_i(x,y;z)$

Since the problems (27)–(29) and (44)–(46) are homogeneous, it is necessary to use an additional condition to support the continuity of the vector functions $\boldsymbol{\chi}^{(1)}(y;z)$ and the matrix elements (53) with respect to the parameter z on the interval $\Omega_z = [z_{\min}, z_{\max}]$. We have used the following additional procedure.

1. At the first point $z = z_1 \in \Omega_z$ the value $y = y_0$ is found, for which the eigenfunction $\psi^{(2)}_i(x_0,y_0;z_1)$ reaches the absolute maximum, and the sign of the eigenfunction $\psi^{(2)}_i(x_0,y_0;z_1)$ is fixed. Here $x_0 \in [x_{\min}, x_{\max}]$ is a fixed point and at least one of the functions $\psi^{(2)}_j(x_0)$ in the expansion (31) is nonzero.

2. At the next points $z \in \Omega_z$ the value of eigenfunction $\psi^{(2)}_i(x_0,y_0;z)$ is calculated and its sign is compared with the the previous one. If they are different, the sign of $\psi^{(2)}_i(x_0,y_0;z)$ is changed and the new value $y = y_0$ is found, for which the eigenfunction $\psi^{(2)}_i(x_0,y_0;z_1)$ reaches the absolute maximum; the sign of the value of eigenfunction $\psi^{(2)}_i(x_0,y_0;z)$ is fixed again.

If the mesh Ω_z is sufficiently dense, the above algorithm works well. Alternatively, one can check the continuity of the coefficients $\chi^{(2)}_{ji}(y;z)$ of the expansion (31) or (32).

4. Benchmark calculations

The efficiency of the above algorithms and programs was demonstrated by the numerical analysis of the parametric 2D BVP solutions, including the evaluation of matrix elements, applied to reduce the 3D BVP describing a helium atom to 1D BVPs for the system of ODEs using the Kantorovich method [13]. The bound-state problem with the steady-state Schrödinger equation for a helium atom with zero total angular momentum in the body-fixed hyperspherical coordinates $x \equiv \theta \in [0,\pi]$, $y \equiv \alpha \in [0,\pi]$, $z \equiv R \in [0,+\infty)$ or $\mathbf{x} = \{x_3 = \theta \succ x_2 = \alpha \succ x_1 = R\}^T \in \mathbf{X} \subset \mathbf{R}^3$ can be formulated as a BVP for the following 3D-elliptic equation

in atomic units [13]:

$$\left(-\frac{1}{R^5}\frac{\partial}{\partial R}R^5\frac{\partial}{\partial R}+\frac{4}{R^2}\left(H(\theta,\alpha;R)+V(\theta,\alpha;R)\right)+2E\right)\Psi(\theta,\alpha,R)=0, \quad (55)$$

$$H(\theta,\alpha;R)=-\frac{1}{\sin^2(\alpha)}\left(\frac{\partial}{\partial\alpha}\sin^2(\alpha)\frac{\partial}{\partial\alpha}+\frac{1}{\sin(\theta)}\frac{\partial}{\partial\theta}\sin(\theta)\frac{\partial}{\partial\theta}\right),$$

$$V(\theta,\alpha;R)=\frac{R}{2}\left(-\frac{2}{\sin(\alpha/2)}-\frac{2}{\cos(\alpha/2)}+\frac{1}{\sqrt{1-\sin(\alpha)\cos(\theta)}}\right).$$

The total wave function $\Psi(\theta,\alpha,R)$ satisfies the following boundary conditions:

$$\lim_{R\to 0}R^5\frac{\partial\Psi(\theta,\alpha,R)}{\partial R}=0, \quad \lim_{R\to\infty}R^5\Psi(\theta,\alpha,R)=0,$$

$$\lim_{\alpha\to 0,\pi}\sin^2(\alpha)\frac{\partial\Psi(\theta,\alpha,R)}{\partial\alpha}=0, \quad \lim_{\theta\to 0,\pi}\sin(\theta)\frac{\partial\Psi(\theta,\alpha,R)}{\partial\theta}=0, \quad (56)$$

and is normalized by the condition

$$\int_0^\infty dRR^5\int_0^\pi d\alpha\sin^2(\alpha)\int_0^\pi d\theta\sin(\theta)\Psi^2(\theta,\alpha,R)=1. \quad (57)$$

As a benchmark let us consider the calculation of the energy for the ground and the first exited states of a helium atom. The calculations were performed with the given accuracy, and their convergence with respect to both the number of the basis vector eigenfunctions and the number of their components was studied.

The 3D BVP for Eq. (55) with the boundary (56) and orthonormalization (57) conditions is reduced to ODEs (11) using the Kantorovich expansion (8) of the desired solutions over the basis functions $\psi_i^{(2)}(\theta,\alpha;R)$ of the 2D BVP (27)–(29). The latter are sought for in the form of expansion (31) over the basis $\psi_i^{(3)}(\theta)$ defined as Legendre polynomials $P_l(\eta=\cos\theta)$, i.e. $U_0(\theta)=0$ in Eq. (33). It means that in the 1D BVP for the resulting ODEs (44)–(46) the potential matrix elements $W_{ij}(\alpha;R)$ from (47) are defined with $V^d=0$.

Figure 1 shows the first four eigenfunctions $\psi_j^{(2)}(\theta,\alpha;R)$ at $\theta=\pi$ and their first derivatives as functions of the hyperradius R and the variable α.

The potential curves $4R^{-2}(\varepsilon_i^{(2)}(R)+1)$, the radial diagonal and nondiagonal matrix elements $H_{ij}^{(1)}(R)$, and the radial matrix elements $Q_{ij}^{(1)}(R)$ versus R are plotted in Fig. 2. As seen from Figs. 1 and 2, our algorithm providing the continuity condition for the eigenfunctions $\psi_i^{(2)}(\theta,\alpha;R)$ works well. The peaks of the matrix elements correspond to the avoided crossings of the potential curves. The classification of potential curves at small and large values of R using the sets of adiabatic quantum numbers (correlation diagram), as well as the asymptotic behavior of matrix elements, is described in Refs. [11, 29].

Numerical calculations demonstrate strict correspondence with theoretical estimates for the eigenvalues, eigenfunctions and their derivatives with respect to the

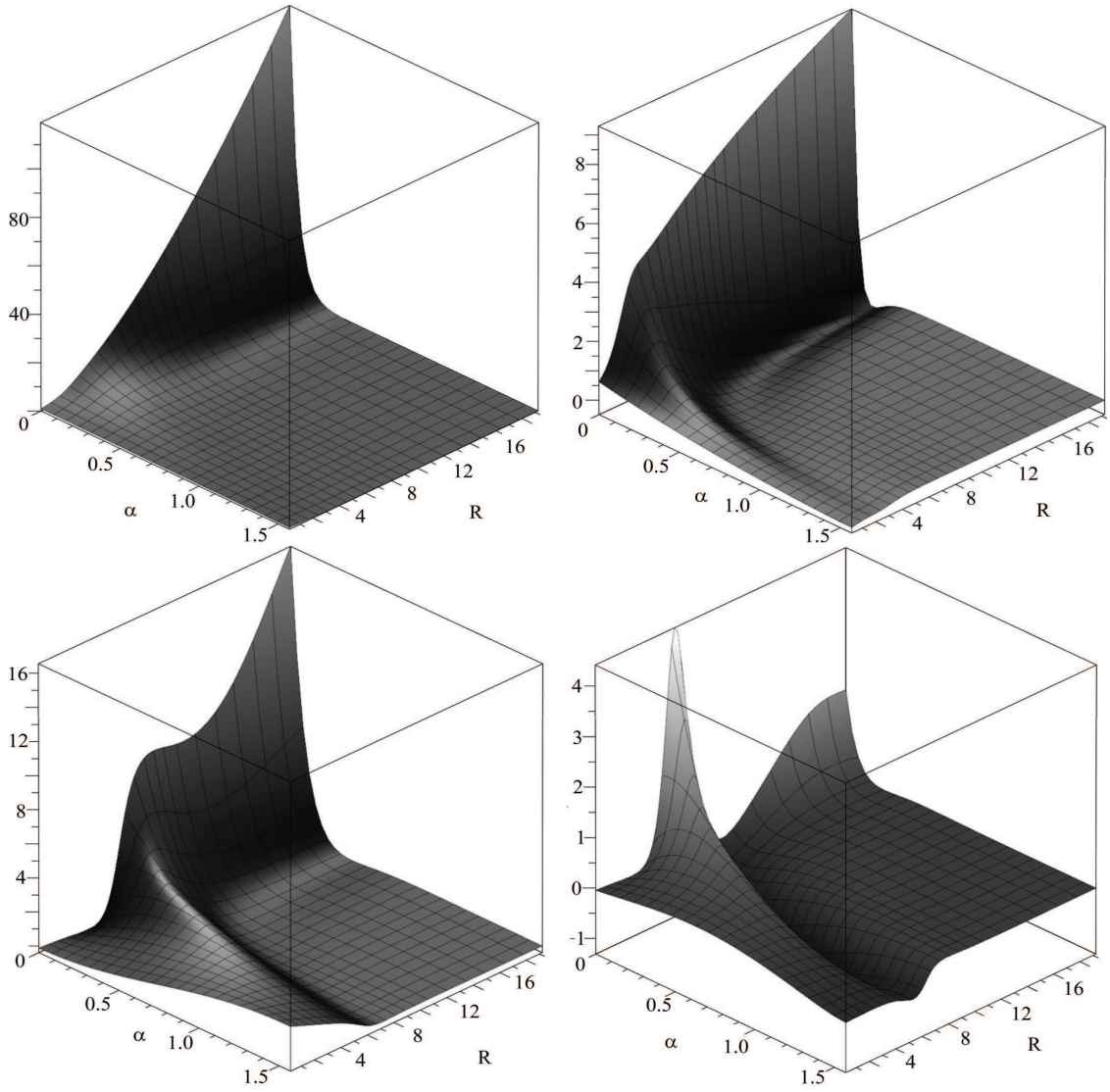

Figure 1: Eigenfunctions $\psi_j^{(2)}(\theta, \alpha; R)$ at $\theta = \pi$ (left) and their first derivatives (right) versus the hyperradius R (a.u.) and the variable α (rad.). Top: $j = 1$. Bottom: $j = 4$.

parameter. In particular, we calculated the Runge coefficients

$$\beta_l = \log_2 \left| \frac{\sigma_l^h - \sigma_l^{h/2}}{\sigma_l^{h/2} - \sigma_l^{h/4}} \right|, \quad l = 1 \div 6. \tag{58}$$

using the absolute errors calculated on four twice-condensed grids for the eigenval-

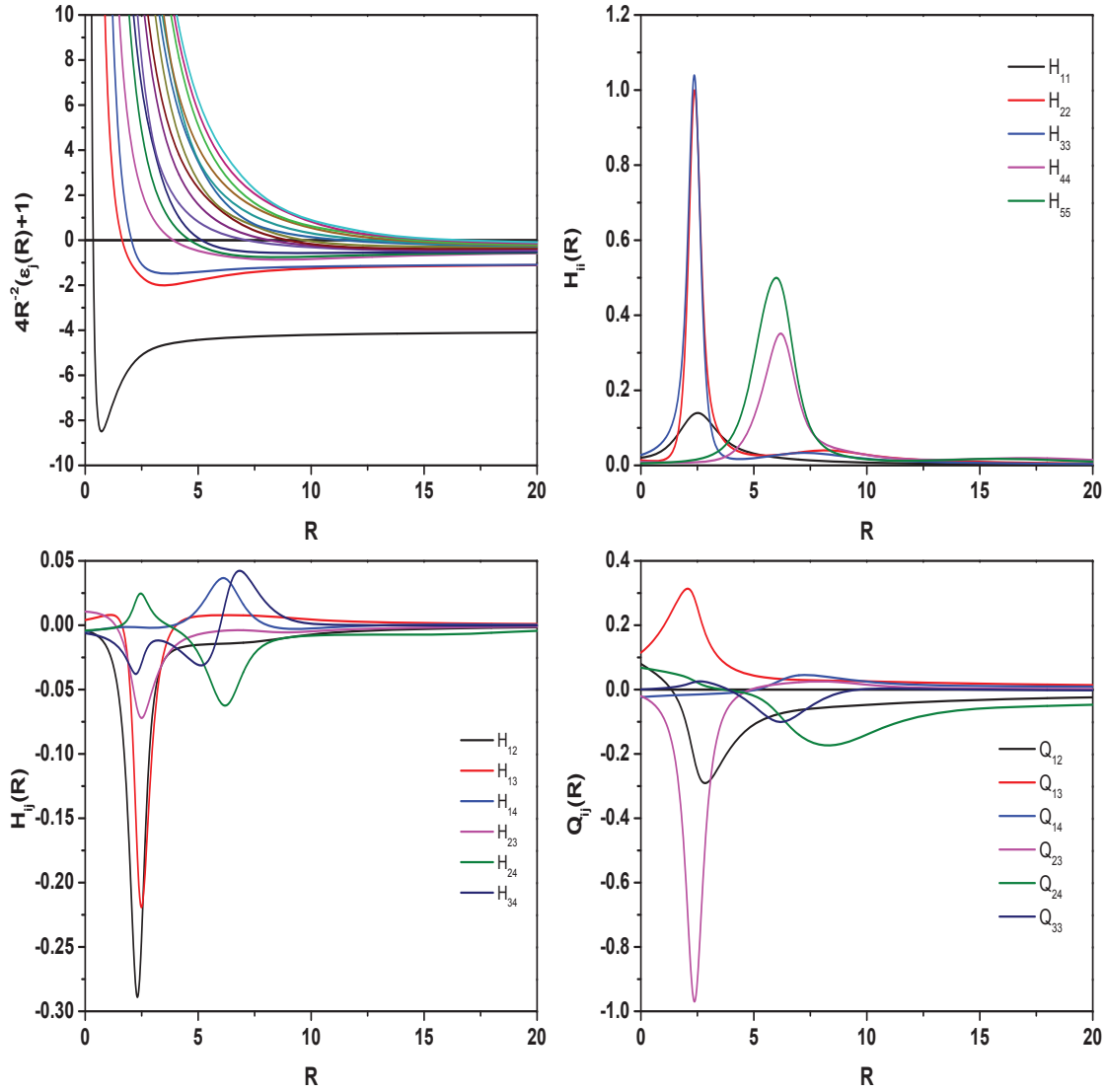

Figure 2: The potential curves $4R^{-2}(\varepsilon_i(R)+1)$ (top-left), the radial diagonal (top-right) and nondiagonal (bottom-left) matrix elements $H_{ij}(R)$, and the radial matrix elements $Q_{ij}(R)$ (bottom-right) versus the hyperradius R

ues, their derivatives, and the matrix elements $H_{ij}^{(1)}(R)$ and $Q_{ij}^{(1)}(R)$:

$$\sigma_1^h = |\varepsilon_j^{h/8(2)}(R) - \varepsilon_j^{h(2)}(R)|, \quad \sigma_3^h = \|\boldsymbol{\chi}_j^{h/8(2)}(\alpha;R) - \boldsymbol{\chi}_j^{h(2)}(\alpha;R)\|_0, \quad (59)$$

$$\sigma_2^h = \left|\frac{\partial\varepsilon_j^{h/8(2)}(R)}{\partial R} - \frac{\partial\varepsilon_j^{h(2)}(R)}{\partial R}\right| \quad \sigma_4^h = \left\|\frac{\partial\boldsymbol{\chi}_j^{h/8(2)}(\alpha;R)}{\partial R} - \frac{\partial\boldsymbol{\chi}_j^{h(2)}(\alpha;R)}{\partial R}\right\|_0,$$

$$\sigma_5^h = |H_{1j}^{h/8(1)}(R) - H_{1j}^{h(1)}(R)|, \quad \sigma_6^h = |Q_{1j}^{h/8(1)}(R) - Q_{1j}^{h(1)}(R)|.$$

Using Eq. (58) we estimated numerically the convergence order of the proposed numerical schemes, the corresponding theoretical estimates being $\beta_l = p+1$, if $l =$

Table 1: Convergence of the potential curves $2R^{-2}(\varepsilon^{(2)}_{43}(R)+1)$, $2R^{-2}(\varepsilon^{(2)}_{45}(R)+1)$ as a function of the maximal number of Legendre polynomials $j_{\max}$ and the number of finite elements $N_{\rm el}$ of the order $p=4$ at $R=7.65$

$j_{\max}$	$N_{\rm el}$	$2R^{-2}(\varepsilon^{(2)}_{43}(R)+1)$	$2R^{-2}(\varepsilon^{(2)}_{45}(R)+1)$
28	6	4.439 005 647 8840	4.879 922 636 3814
28	12	4.438 991 442 6147	4.878 939 387 2213
28	18	4.438 991 281 3574	4.878 936 678 0110
28	24	4.438 991 270 2793	4.878 936 575 2142
28	30	4.438 991 268 8569	4.878 936 565 5674
28	36	4.438 991 268 5908	4.878 936 564 0653
40	36	4.438 814 541 3791	4.878 929 789 5129
50	36	4.438 775 794 7833	4.878 928 117 4560
60	36	4.438 759 636 3135	4.878 927 388 1689
70	36	4.438 751 689 2542	4.878 927 020 3953
80	36	4.438 747 322 9410	4.878 926 815 1861
100	36	4.438 743 080 9327	4.878 926 613 2176
120	36	4.438 741 240 5373	4.878 926 524 5981

Table 2: Convergence of the matrix elements $Q^{(1)}_{4345}(R)$, $H^{(1)}_{4345}(R)$, $H^{(1)}_{4545}(R)$ at $R=7.65$, similar to Table 1

$j_{\max}$	$N_{\rm el}$	$Q^{(1)}_{4345}(R), 10^{-3}$	$H^{(1)}_{4345}(R), 10^{-4}$	$H^{(1)}_{4545}(R), 10^{-3}$
28	6	7.163 551 693 508	1.313 245 172 874	1.034 074 714 010
28	12	7.192 416 552 701	1.313 393 326 976	1.037 535 372 894
28	18	7.192 470 461 759	1.313 394 061 373	1.037 544 063 945
28	24	7.192 471 802 131	1.313 393 807 683	1.037 544 380 393
28	30	7.192 471 876 618	1.313 393 761 626	1.037 544 409 101
28	36	7.192 471 882 307	1.313 393 751 746	1.037 544 413 457
40	36	7.164 925 249 674	1.304 767 510 954	1.036 946 196 503
50	36	7.158 600 336 853	1.302 825 852 351	1.036 806 107 806
60	36	7.155 920 393 086	1.302 012 009 221	1.036 746 299 243
70	36	7.154 591 453 293	1.301 611 523 137	1.036 716 518 763
80	36	7.153 857 856 101	1.301 391 714 358	1.036 700 039 417
100	36	7.153 142 578 776	1.301 178 645 274	1.036 683 940 956
120	36	7.152 831 407 895	1.301 086 493 836	1.036 676 926 529

$3, 4$, and $\beta_l = 2p$ otherwise. Within the chosen approximation order $p=4$ we got the numerical estimate $7.5 \div 7.8$ of the Runge coefficients β_l for the eigenvalues, their derivatives, and the matrix elements, and $4.6 \div 4.8$ for the eigenfunctions and their

Table 3: The disk storage usage (DSU, KB) and the CPU time (min:sec) scale with the number $j_{\max}$ of equations, the number $n = N_{\rm el}$ and order p of the finite-elements and the number N of eigensolutions, number of iterations NITEM, and minimal dimensions MTOT and MITOT of working arrays TOT and ITOT, respectively, and CPU time per iteration (TCPU) (sec) at the convergence tolerance on eigenvalues RTOL $= 10^{-12}$ and the lower bound of lowest eigenvalue SHIFT=-1.1.

$j_{\max}$	$n = N_{\rm el}$	p	N	MTOT	MITOT	CPU	DSU	NITEM	TCPU
12	6	4	6	33914	1300	<0:01	912	45	<0.01
12	6	4	12	33914	1306	<0:01	3304	52	<0.01
12	6	8	6	108242	2476	0:10	4884	43	0.23
28	6	4	6	182874	2980	0:22	4644	45	0.49
28	6	4	12	182874	2986	0:26	4816	52	0.50
28	6	8	6	585330	5692	1:32	8232	43	2.14
12	36	4	6	162548	7570	0:24	4528	47	0.51
28	36	4	6	768708	17410	2:49	9440	47	3.60
28	36	4	12	826122	17416	3:23	10720	52	3.90

derivatives. These results correspond to the theoretical error estimates at the fixed number $j_{\max}$ of the equations. The calculations using Eqs. (59) were performed with the specified accuracy of $\sim 10^{-12}$ by means of the POTHEA program with the relative error tolerance $\epsilon_1 = 4 \cdot 10^{-16}$ for the calculated eigenvalues. We used the computer 2 x Xeon 3.2 GHz, 4 GB RAM, Intel Fortran 77, and the data type real*8 that provides 16 significant digits. The running time in this example was 2 seconds for $j_{\max} = 12$, $N = 6$ and 1000 seconds for $j_{\max} = 50$, $N = 50$.

The convergence of several matrix elements with respect to the number of the Legendre polynomials $j_{\max} = 12, 28, 40, 50, 60, 70, 80, 100, 120$ and the number of finite elements $N_{\rm el} = 6, 12, 18, 24, 30, 36$ of the grid $\Omega_\alpha = \{0(N_{\rm el})\pi/2\}$ at $p = 4$ is shown in Tables 1–2. The potential curves $2R^{-2}(\varepsilon_j^{(2)}(R) + 1)$ and the matrix elements $H_{ij}^{(1)}(R)$ converge monotonically from above with the growth of $N_{\rm el}$ and $j_{\max}$. The absolute values of the matrix elements $Q_{ij}^{(1)}(R)$ converge monotonically from above with increasing $j_{\max}$ and from below with increasing $N_{\rm el}$.

As seen from Tables 1–2, the convergence of eigenvalues and matrix elements depending on the number of Legendre polynomials $P_{j-1}(\eta = \cos\theta)$ is proportional to j^{-3}. This fact is explained by the properties of the symmetric potential $j_{\max} \times j_{\max}$ matrices $\mathbf{W}^{(2)}(\alpha; R)$ from Eq. (47):

$$= \int_{-1}^{1} d\eta \frac{P_{i-1}(\eta) P_{j-1}(\eta)}{\sqrt{1 - \sin(\alpha)\eta}}, \quad \eta = \cos\theta. \tag{60}$$

Because of the symmetry of the matrix elements $W_{ij}(\alpha; R)$ with respect to $\alpha = \pi/2$, the problem (60) should be restricted to $\alpha \in [0, \pi/2]$ with the following boundary

Table 4: Convergence of the ground state energy (in a.u.) for helium atom depending on the number N of basis functions and the number $j_{\max}$ of the Legendre polynomials

N	$j_{\max}=12$ [13]	$j_{\max}=12$	$j_{\max}=21$	$j_{\max}=28$
1	−2.887 911 68	−2.895 539 19	−2.895 551 19	−2.895 552 76
2	−2.891 379 91	−2.898 631 57	−2.898 643 21	−2.898 644 74
6	−2.903 004 48	−2.903 644 06	−2.903 655 96	−2.903 657 52
10	−2.903 636 13	−2.903 702 86	−2.903 714 79	−2.903 716 36
15	−2.903 705 49	−2.903 708 67	−2.903 720 60	−2.903 722 16
21	−2.903 722 64			−2.903 722 99
28	−2.903 722 66			
N	$j_{\max}=35$	$j_{\max}=40$	$j_{\max}=45$	$j_{\max}=50$
1	−2.895 553 32	−2.895 553 52	−2.895 553 63	−2.895 553 71
2	−2.898 645 28	−2.898 645 47	−2.898 645 58	−2.898 645 66
6	−2.903 658 08	−2.903 658 27	−2.903 658 39	−2.903 658 46
10	−2.903 716 91	−2.903 717 10	−2.903 717 22	−2.903 717 30
15	−2.903 722 72	−2.903 722 91	−2.903 723 03	−2.903 723 10
21	−2.903 723 54	−2.903 723 74	−2.903 723 85	−2.903 723 93
28	−2.903 723 55	−2.903 723 74	−2.903 723 85	−2.903 723 93
35		−2.903 723 91	−2.903 724 03	−2.903 724 10
40			−2.903 724 03	−2.903 724 10
45				−2.903 724 15
[12]				−2.903 722 99
[31]				−2.903 724 37

conditions for the ground and the first exited states:

$$\lim_{\alpha\to 0,\pi/2} \sin^2(\alpha)\frac{\partial \boldsymbol{\chi}^{(2)}(\alpha;R)}{\partial\alpha} = 0. \tag{61}$$

The 1D weakly singular integral (60) is usually calculated analytically using Clebsch-Gordan coefficients [30, 12]. This approach suffers from significant numerical errors at large i and j that arise from calculating the factorials of large numbers (the factorials of up to $4j_{\max}-3$ are required). After the change of variable in Eq. (60)

$$\eta(\zeta;\alpha) = \frac{\tan(\alpha/2)}{2}(1-\zeta^2)+\zeta, \quad \zeta\in[-1,1], \quad \alpha\in[0,\pi/2], \tag{62}$$

we arrive at the nonsingular integral

$$W_{ij}^{rep}(\alpha) = W_{ij}^{rep}(\pi-\alpha) = \frac{1}{\cos(\alpha/2)}\int_{-1}^{1} d\zeta P_{i-1}(\eta(\zeta;\alpha))P_{j-1}(\eta(\zeta;\alpha)). \tag{63}$$

This 1D integral was calculated using the 96-order Gauss–Legendre quadrature, which yields the double-precision accuracy $\le 10^{-14}$ at $i,\, j \le 50$. Indeed, as follows

Table 5: Convergence of the first exited state energy (in a.u.), similar to Table 4

N	$j_{\max}=21$	$j_{\max}=28$	$j_{\max}=35$
1	−2.139 935 59	−2.139 935 68	−2.139 935 71
2	−2.141 664 27	−2.141 664 32	−2.141 664 34
6	−2.145 700 08	−2.145 700 17	−2.145 700 20
10	−2.145 914 95	−2.145 915 04	−2.145 915 07
15	−2.145 957 21	−2.145 957 30	−2.145 957 34
21		−2.145 968 71	−2.145 968 74
28			−2.145 970 24
N	$j_{\max}=40$	$j_{\max}=45$	$j_{\max}=50$
1	−2.139 935 72	−2.139 935 72	−2.139 935 73
2	−2.141 664 35	−2.141 664 35	−2.141 664 36
6	−2.145 700 21	−2.145 700 21	−2.145 700 22
10	−2.145 915 09	−2.145 915 09	−2.145 915 10
15	−2.145 957 35	−2.145 957 36	−2.145 957 36
21	−2.145 968 76	−2.145 968 76	−2.145 968 77
28	−2.145 970 26	−2.145 970 26	−2.145 970 27
35	−2.145 972 10	−2.145 972 10	−2.145 972 11
40		−2.145 972 62	−2.145 972 63
45			−2.145 973 22
[12]			−2.145 956 97
[32]			−2.145 974 04

from the estimates for the matrix elements $W^{rep}_{i\ll j}(\alpha) \sim 1/\sqrt{j}$ (in particular, for the integral (60) at $i=1$),

$$W^{rep}_{1j}(\alpha) = 2\exp(-(j-1/2)\mathrm{arch}(\sin^{-1}\alpha))/(\sqrt{2j-1}\sqrt{\sin\alpha}),$$

and $\varepsilon^{(3)}_{j-1} = (j-1)j \sim j^2$, which yields an estimate for the correction of eigenvalues $\delta\varepsilon \sim j^{-3}$ in the second-order perturbation theory. This means that the accuracy of the calculations $\sim 10^{-12}$ will be achieved with $j_{\max}$ being at least ~ 1500 .

Table 3 shows the disk storage usage (DSU) and the CPU time at different values of the number of equations $j_{\max}$, the number $n = N_{\mathrm{el}}$ and the order p of finite elements, and the number N of eigensolutions. The minimal dimensions MTOT and MITOT of the working arrays TOT and ITOT used in the test run of calculations of matrix potentials are also presented. The relative error tolerance was $\epsilon_2 = 10^{-12}$. The calculations were performed using Intel Core i5 CPU 3.33 GHz, 4 GB RAM, Windows 7. The execution time is seen to be proportional to the number of calculated solutions and quadratically dependent on the number of equations, or the number of nodal points $L+1 = np+1$, while the disk storage usage is slowly dependent on the number of calculated solutions and quadratically dependent on the number of equations (nodal points). This follows from exploiting the banded structure of the system of $(N_{\mathrm{el}} \cdot p + 1) \cdot j_{\max}$ linear algebraic equations with the

maximum band half-width $(p+1)\cdot j_{\max}$; the number of arithmetic operations of the appropriate SSPACE subroutine is specified in Ref. [33].

In the benchmark calculations the grids in R and α have been chosen as $\Omega_R = \{0(200)10(200)30\}$ and $\Omega_\alpha = \{0(150)\pi/2\}$. Enclosed in parentheses are the numbers of finite elements of the order $p = 4$ in each interval. The set of matrix elements including the eigenfunction with the number $N = 50$ were calculated with the accuracy 10^{-8} using the number of finite elements $N_{\rm el} = 150$ at $\epsilon_2 = 10^{-12}$. The banded system of $(150 \times 4 + 1) \times 50 = 30050$ linear algebraic equations with the mean bandwidth $(4+1) \times 50 = 250$ was stably solved with the relative error tolerance $\epsilon_2 = 10^{-12}$ at each value of the hyperradius R belonging to the set of Gaussian nodes of the grid Ω_R.

The convergence of energy values for helium atom in the ground and the first exited states depending on the number N of radial equations and the number $j_{\max}$ of the Legendre polynomials is demonstrated in Tables 4 and 5. The energy eigenvalues converge monotonically from above, achieving the values $E_1 = -2.903\,724\,15$ a.u. and $E_2 = -2.145\,973\,22$ a.u. at $N = 45$, $j_{\max} = 50$. At $j_{\max} \sim N$ the obtained results agree within the accuracy of 10^{-6} with the variational estimates [31, 32] and have higher accuracy than the earlier calculations [13, 12]. With the appropriate asymptotic behavior of the matrix elements and solutions taken into account [12], a similar accuracy can be achieved in higher excited states of the helium atom, to which the variational calculations were not applied.

5. Results and prospects

The software packages KANTBP, ODPEVP, and POTHEA allow the prescribed-accuracy solution of the boundary-value problem for a 2D or 3D elliptic-type equation within the framework of Kantorovich method with discretization of the sequence of boundary-value problems. The software package POTHMF is intended for numerical solution of the problems **1**–**3** with angular oblate spheroidal functions.

The efficiency of the developed methods, algorithms, and software packages KANTBP [5, 6, 7], POTHMF [27], ODPEVP [8] and POTHEA [28] is confirmed by the results of numerical testing of theoretically derived estimates for the boundary-value solution errors and by the results of simulation of the following physical processes in few-body quantum systems.

Numerical studies of the resonance photoionization and laser-stimulated recombination of a hydrogen atom in a uniform magnetic field were carried out. The effects of resonance transmission and total reflection of oppositely charged particles in a uniform magnetic field were predicted for the first time [17, 19].

For the model of axial channelling of similarly charged particles in the effective confining oscillator potential of a crystal the numerical study was carried out. The simulations revealed a non-monotonic dependence of the nuclear reaction rate enhancement coefficient $K(E)$ upon the collision energy E due to the newly discovered resonance effects in the transmission and reflection of channelled ions [20, 21].

Sybmolic-numeric modeling was carried out for the tunneling of a cluster through repulsive potential barriers in s-wave approximation. The cluster model consists of a pair of particles or ions, or several identical particles, coupled by pair short-range potentials of the oscillator type. The study revealed non-monotonic dependence of the reflection and transmission coefficients upon the collision energy, as well as the particle number and symmetry type of the cluster state. It was shown that the resonance transmission of the cluster through the barriers, i.e., the quantum transparency effect, accompanied with characteristic increase of the probability density in the vicinity of local minima of the potential energy with respect to the transverse variables, is a manifestation of metastable states of the cluster arising due to its interaction with barriers [22, 23, 24].

The above symbolic-numeric technique was also applied to the analysis of spectral and optical properties of electronic and impurity states of axially-symmetric models of semiconductor quantum wells, quantum wires and quantum dots. These states were calculated in the effective mass approximation in the presence of external fields, including quantum-dimensional Zeeman and Stark effects [10, 18].

The calculation of parametric eigenvalues, eigenfunctions, and matrix elements of the BVPs for Eqs. (44) and (39) using POTHEA [9, 8] can be applied to the numerical solution with the required accuracy of bound-state and scattering problems with 3D Schrödinger-type equations, including those with long-range Coulomb-type potentials. With the help of KANTBP [5, 6, 7] they can be applied to various three-dimensional elliptic equations in partial derivatives. The generalization of the algorithm over a system of parametric coupled 2D BVPs in the framework of the projection method and FEM, which can be applied to solving multidimensional boundary-value problems with Schrödinger-type equations, will be presented in forthcoming papers.

Presently in progress is the final version **POTHEA 2.0** for solving the problem with respect to unknowns, which implies the calculation of improved parametric basis functions in K form (44)–(46) and (48)–(52) using the algorithm MPKM of Section 2.

A generalization of the multiparametric Kantorovich method implying the reduction to $2N-1$ multiparametric eigenvalue problems for a set of $\sim 10-50$ ordinary second-order differential equations that can be solved with respect to $N-1$, $N-2$, ..., 1, 0 independent parameters using MPI and/or GRID technology is also planned.

References

[1] Born M. and Oppenheimer J.R. *Zur quantentheorie der molekeln.* Annalen der physik 1927, **84**, pp. 457–484

[2] Born M. and Huang K. *Dynamical theory of crystal lattices.* 1954, Oxford: Clarendon

[3] Wheeler J.A. *On the mathematical description of light nuclei by the method of resonating group structure*. Phys. Rev. 1937, **52**, pp. 1107–1122

[4] Kantorovich L.V. and Krylov V.I. *Approximate methods of higher analysis*. 1964, New York: Wiley

[5] Chuluunbaatar O., Gusev A.A., Abrashkevich A.G., Amaya-Tapia A., Kaschiev M.S., Larsen S.Y., Vinitsky S.I. *KANTBP: A program for computing energy levels, reaction matrix and radial wave functions in the coupled-channel hyperspherical adiabatic approach*. Comput. Phys. Commun. 2007, **177**, pp. 649–675; http://cpc.cs.qub.ac.uk/summaries/ADZH_v1_0.html

[6] Chuluunbaatar O., Gusev A.A., Vinitsky S.I. and Abrashkevich A.G. *KANTBP 2.0: New version of a program for computing energy levels, reaction matrix and radial wave functions in the coupled-channel hyperspherical adiabatic approach*. Comput. Phys. Commun. 2008, **179**, pp. 685–693; http://cpc.cs.qub.ac.uk/summaries/ADZH_v2_0.html

[7] Chuluunbaatar O., Gusev A.A., Vinitsky S.I. and Abrashkevich A.G. *KANTBP 3.0: New version of a program for computing energy levels, reflection and transmission matrices, and corresponding wave functions in the coupled-channel adiabatic approach*. Lib JINR, 2013; http://wwwinfo.jinr.ru/programs/ jinrlib/kantbp/indexe.html.

[8] Chuluunbaatar O., Gusev A.A., Vinitsky S.I. , Abrashkevich A.G. *ODPEVP: A program for computing eigenvalues and eigenfunctions and their first derivatives with respect to the parameter of the parametric self-adjoined Sturm-Liouville problem*. Comput. Phys. Commun. 2009, **180**, pp. 1358–1375; http://cpc.cs.qub.ac.uk/summaries/AEDV_v1_0.html

[9] Gusev A.A.,Chuluunbaatar O., Vinitsky S.I., Abrashkevich A.G. *POTHEA: A program for computing eigenvalues and eigenfunctions and their first derivatives with respect to the parameter of the parametric self-adjoined 2D elliptic partial differential equation*. Comput. Phys. Commun. 2014 (accepted); http://cpc.cs.qub.ac.uk/summaries/ADZH_v2_0???.html

[10] Gusev A.A., Chuluunbaatar O., Gerdt V.P., Rostovtsev V.A., Vinitsky S.I., Derbov V.L., Serov V.V., *Symbolic-numeric algorithms for computer analysis of spheroidal quantum dot models*. LNCS 2010, **6244**, pp. 106-122; http://arxiv.org/abs/1004.4202

[11] Abrashkevich A.G., Abrashkevich D.G., Puzynin I.V., Vinitsky S. I., *Adiabatic hyperspherical representation in barycentric coordinates for helium-like systems* J. Phys. B 1991, **24**, pp. 1615-1638.

[12] De Groote J.J., Masili M., Hornos J.E., *Highly excited states for the helium atom in the hyperspherical adiabatic approach*. J. Phys. B 1998, **31**, pp. 4755–4764

[13] Abrashkevich A.G., Kaschiev M.S., Vinitsky S.I. *A new method for solving an eigenvalue problem for a system of three Coulomb particles within the hyperspherical adiabatic representation*. J. Comput. Phys. 2000, **163**, pp. 328–348

[14] Dubovik V.M., Markovski B.L., Vinitsky S.I. *Multistep adiabatic approximation*. Preprint JINR E4-87-743, Dubna, 1987;
http://www-lib.kek.jp/cgi-bin/img_index?8801189

[15] Gusev A.A., Chuluunbaatar O., Gerdt V.P., Markovski B.L., Serov V.V., Vinitsky S.I. *Algorithm for reduction of boundary-value problems in multistep adiabatic approximation*. arXiv:1005.2089

[16] Makarewicz J. *Adiabatic multi-step separation method and its application to coupled oscillators*. Theor. Chim. Acta 1985, **68**, pp. 321–334

[17] Chuluunbaatar O., Gusev A.A., Derbov V.L., Kaschiev M.S., Melnikov L.A., Serov V.V. and Vinitsky S.I. *Calculation of a hydrogen atom photoionization in a strong magnetic field by using the angular oblate spheroidal functions*. J. Phys. A 2007, **40**, pp. 11485-11524

[18] Vinitsky S.I., Chuluunbaatar O., Gerdt V.P., Gusev A.A., and Rostovtsev V.A. *Symbolic-numerical algorithms for solving parabolic quantum well problem with hydrogen-like impurity*. Lect. Notes in Computer Sci. 2009, **5743**, pp. 334-349.

[19] Chuluunbaatar O., Gusev A.A., Derbov V.L., Kaschiev M.S., Mardoyan L.G., Serov V.V., Tupikova T.V. and Vinitsky S.I. *Adiabatic representation for a hydrogen atom photoionization in an uniform magnetic field*. Phys. Atom. Nucl. 2008, **71**, pp. 844–852

[20] Chuluunbaatar O., Gusev A.A., Derbov V.L., Krassovitskiy P.M. and Vinitsky S.I. *Channeling problem for charged particles produced by confining environment*. Phys. Atom. Nucl. 2009, **72**, pp. 768–778

[21] Vinitsky S.I., Gusev A.A., Chuluunbaatar O., Derbov V.L., Serov V.V. and Krassovitskiy P.M. *Effects of resonant transmission and reflection of channeled ions in presence of a transverse oscillator potential*. Proc. of International Conference "Modeling Nonlinear processes and systems", ed. L.A. Uvarova, MSTU STANKIN, M., Janus-K, 2009, bf 12, pp. 402 - 422. (in Russian)

[22] Gusev A.A., Chuluunbaatar O.,Gerdt V.P., Rostovtsev V.A., Vinitsky S.I. *Symbolic-numerical algorithms to solve the quantum tunneling problem for a coupled pair of ions*. Lect. Notes Comp. Sci. 2011, **6885**, pp. 175-191

[23] Gusev A.A., Vinitsky S.I., Chuluunnbaatar O., Krassovitskiy P.M. *The resonance tunneling of coupled pair of particles in adiabatic representation*. Vestnik MSTU "STANKIN" 2013, No 1 (24), pp. 92–97 (in Russian)

[24] Vinitsky S., Gusev A., Chuluunbaatar O., Rostovtsev V., Hai L.L., Derbov V., Krassovitskiy P., *Symbolic-numerical algorithms for generating cluster eigenfunctions: tunneling of clusters through repulsive barriers*. Lect. Notes Comp. Sci. 2013, **8136**, pp. 427–442

[25] Chuluunbaatar O. *Variational-iteration algorithms of numerical solving bound state and scattering problems for coupled-channels radial equations*. Bulletin of PFUR. Math. Comp. Sci. Phys. 2008, No 2, pp. 40–56 (in Russian)

[26] Chuluunbaatar O. *Algorithm of numerical solving the parametric sturm-liouville problem and calculation of solution derivatives with respect to the parameter via the finite-element method*. Bulletin of PFUR. Math. Comp. Sci. Phys. 2009, No 2, pp. 54–65 (in Russian)

[27] Chuluunbaatar O., Gusev A.A., Gerdt V.P., Rostovtsev V.A., Vinitsky S.I., Abrashkevich A.G., Kaschiev M.S. and Serov V.V. *POTHMF: A program for computing potential curves and matrix elements of the coupled adiabatic radial equations for a hydrogen-like atom in a homogeneous magnetic field*. Comput. Phys. Commun. 2008, **178**, pp. 301–330; http://cpc.cs.qub.ac.uk/summaries/AEAA_v1_0.html

[28] Gusev A.A. *The algorithms of the numerical solution to the parametric two-dimensional boundary-value problem and calculation derivative of solution with respect to the parameter and matrix elements by the finite-element method*. Bulletin of PFUR. Math. Comp. Sci. Phys. 2013, No 4, pp. 101–121

[29] Abrashkevich A.G., Puzynin I.V., Vinitsky S.I. *ASYMPT: a program for calculating asymptotics of hyperspherical potential curves and adiabatic potentials*. Comput. Phys. Commun. 2000, **125**, pp. 259–281; http://cpc.cs.qub.ac.uk/summaries/ADLL_v1_0.html

[30] Abrashkevich A.G., Abrashkevich D.G., Shapiro M., *HSTERM — A program to calculate potential curves and radial matrix elements for two-electron systems within the hyperspherical adiabatic approach*. Comput. Phys. Comm. 1995, **90**, pp. 311–339; http://cpc.cs.qub.ac.uk/summaries/ADBZ_v1_0.html

[31] Chuluunbaatar O., Puzynin I.V. and Vinitsky S.I. *Uncoupled correlated calculations of helium isoelectronic bound states*. J. Phys. B 2001, **34** pp. L425–L432.

[32] Drake G.W.F. and Zong-Chao Van *Variational eigenvalues for the S states of helium*. Chem. Phys. Lett. 1994, **229**, pp. 486–490

[33] Bathe K.J. *Finite element procedures in engineering analysis*. 1982, New York: Englewood Cliffs, Prentice Hall